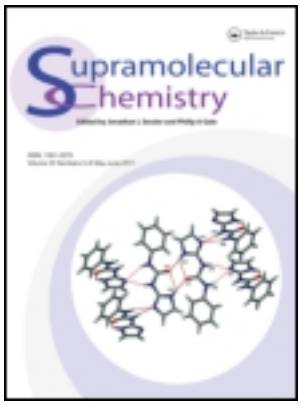

Supramolecular Chemistry
Publication details, including instructions for authors and subscription information:
http://www.tandfonline.com/loi/gsch20

Insights into the photophysics, protonation and Cu^{2+} ion coordination behaviour of anthracene-9,10-dione-based chemosensors

Navneet Kaur [a] & Subodh Kumar [b]

[a] Department of Chemistry, Panjab University, Chandigarh, 160 014, Punjab, India

[b] Department of Chemistry, Guru Nanak Dev University, Amritsar, 143 005, Punjab, India

Available online: 03 Nov 2011

To cite this article: Navneet Kaur & Subodh Kumar (2011): Insights into the photophysics, protonation and Cu^{2+} ion coordination behaviour of anthracene-9,10-dione-based chemosensors, Supramolecular Chemistry, 23:11, 768-776

To link to this article: http://dx.doi.org/10.1080/10610278.2011.622386

Supramolecular Chemistry
Vol. 23, No. 11, November 2011, 768–776

Insights into the photophysics, protonation and Cu^{2+} ion coordination behaviour of anthracene-9,10-dione-based chemosensors

Navneet Kaur[a]* and Subodh Kumar[b1]

[a]*Department of Chemistry, Panjab University, Chandigarh 160 014, Punjab, India;* [b]*Department of Chemistry, Guru Nanak Dev University, Amritsar 143 005, Punjab, India*

(*Received 21 May 2011; final version received 1 September 2011*)

Carboxylic acid–diamine-based Cu^{2+} chromogenic sensors (**3** and **4**) exhibited colour switching from red to blue with good sensitivity and selectivity towards Cu^{2+} among other physiologically important alkali, alkaline earth and heavy metal ions. This colour-switching phenomenon arises due to selective deprotonation of aryl amine NH by Cu^{2+}. Significantly, chemosensor **3** (λ_{max} 492 nm) shows multiple modes of complexation towards Cu^{2+}. It is very much evident from the appearance of blue colour (λ_{max} 615 nm) at pH $>$ 7.0 and yellow colour (λ_{max} 465 nm) at pH $<$ 4.0. In addition, chemosensor **3** exhibits a unique logic gate system that involves 'INHIBIT' and 'TRANSFER' logic gates.

Keywords: chromogenic sensor; anthracene-9,10-dione; stoichiometry; stability constant; pH; logic gates

1. Introduction

Investigation of well-defined small-molecule receptors, which give rise to visible or luminescent changes upon interaction with metal ions/anions/neutral species, continue unabated, as new chemosensing platforms are synthesised and explored (*1–4*). Industrial processes often demand detection methods that require sophisticated instrumentation such as atomic absorption/emission spectrometry or inductively coupled plasma mass spectroscopy (*5*). These analytical techniques are not very suitable for fast detection protocols. Therefore, it is important to develop methods allowing rapid, straightforward analyte detection. In this regard, colorimetric sensors offer an advantage of providing information with minimal equipment allowing the so-called naked-eye detection. There are numerous examples of colorimetric probes for anionic and cationic species (*6*). Common drawbacks of these systems are that they often require complicated synthesis and their design is not flexible. Therefore, every analyte requires its own probe design.

Since metal ions can have detrimental effects on humans and the environment, the development of highly selective sensors for metal ions is particularly important (*7*). Copper is the third most abundant essential trace element in the human body and is commonly found as Cu^{2+} in natural water (*8*). However, free Cu^{2+} is potentially very toxic to aquatic life, both acutely and chronically. For example, micro-organisms are affected by even submicromolar concentrations of Cu^{2+} (*9*). The excessive uptake of copper causes liver or kidney damage (*10*). Several analytical methods (*11*) and a number of probes (*12*, *13*) have been developed for sensitive, selective and accurate detection of Cu^{2+}. Colorimetric methods, in particular, are often attractive because they can be easily detected with the naked eye. Most of the reported sensors for Cu^{2+} are used in mixed solvent (water/organic solvent). But, only a few of them have the potential to be used in neat aqueous solution (*13f*). Significance of the development of naked-eye sensors for Cu^{2+} that are freely soluble in neat aqueous solution lies in the fact that they can be used to evaluate the analyte concentration rapidly.

Versatile chemical input–optical output features are of much significance and have been widely applied in two closely related fields: molecular chemosensing and molecular scale 'logic gates'. In the former, optical signals are used to detect the presence of certain chemical species in solution (*14*). In the second approach, chemical species are treated as inputs that control through the Boolean logic rules, the output, is usually a light signal (*15*). In the chemosensing field, the goal is often selectivity, that is, a unique chemical species that induce a unique change in colour or fluorescence. In contrast, molecular logic looks for more complex systems, which usually contain multiple binding sites and show certain unique response patterns, exemplifying the desired logic operation in the presence of either or both inputs.

1-Aminoanthracene-9,10-dione, a chromogenic moiety, has been successfully used for designing anion sensor (*16*), where NH deprotonation leads to colour changes. We envisaged that the presence of an appropriate metal interacting unit in the 1-aminoanthracene-9,10-dione unit

*Corresponding author. Email: neet_chem@yahoo.co.in

ISSN 1061-0278 print/ISSN 1029-0478 online

http://dx.doi.org/10.1080/10610278.2011.622386
http://www.tandfonline.com

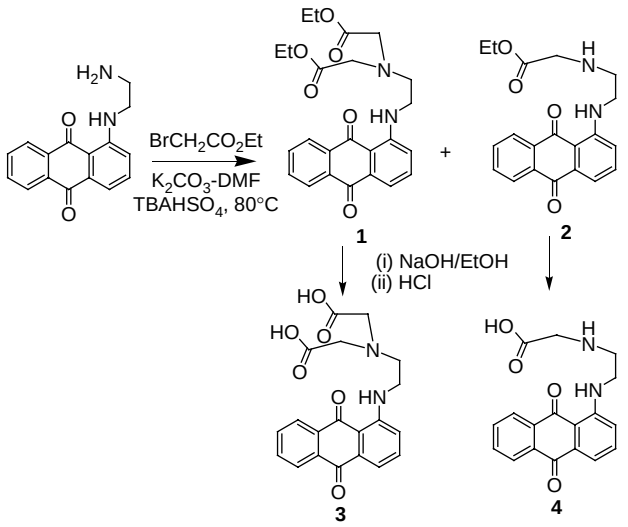

Scheme 1. Synthesis of chemosensors 3 and 4.

would induce metal-mediated colour changes, enabling chromogenic metal ion sensors with bathochromic shifts (*17*). Similar type of deprotonation has been observed in naphthalimide-based chemosensors (*18*).

Earlier studied anthracene-9,10-dione-based chemosensors were insoluble in water and as a result mixed solvent mixture (CH_3OH:H_2O) has to be used for their photophysical studies. Therefore, these chemosensors could not be used in neat aqueous solution – a prerequisite for their use in biological environment. In order to develop direct usability of such chemosensors, in addition to selectivity, their solubility and stability features need to be addressed. The presence of hydrophilic non-coordinating groups in the amine nitrogen is expected to increase the solubility of the respective chemosensor in water or aqueous buffer and would provide opportunities for the estimation of Cu^{2+} under biological environments. Accordingly, we have designed and synthesised chemosensor **3** for transition metal ion estimation and have found that the chemosensor **3** (λ_{max} 492 nm) shows multiple modes of complexation towards Cu^{2+}. It is evident from the appearance of blue colour (λ_{max} 615 nm) at pH >7.0 and yellow colour (λ_{max} 465 nm) at pH <4.0. In addition, these various output patterns have been used for the elaboration of molecular scale logic gates.

2. Synthesis of chemosensors 3 and 4

2-Aminoethylaminoanthracene-9,10-dione (*17a*) on alkylation with ethyl bromoacetate in CH_3CN–K_2CO_3–TBA·HSO_4 system provided the mixture of diester **1** [higher R_f component, red solid; 60%; m.p. 78°C (CH_2Cl_2); FAB mass M^+*m/z* 439 ($M^+ + 1$)] and monoester **2** [lower R_f component, red solid; 30%; m.p. 68°C (CH_2Cl_2); FAB mass M^+*m/z* 353 ($M^+ + 1$); CH_2Cl_2; Scheme 1], which were purified by column chromatography and re-crystallisation. Diester **1** on hydrolysis with ethanolic NaOH solution followed by acidification gave diacid **3**, red solid.

Similarly, monoester **2** on hydrolysis with ethanolic NaOH solution followed by acidification gave monoacid **3** (Scheme 1). Structures of **1**–**4** have been confirmed by ^{1}H NMR, ^{13}C NMR, mass spectral data and CHN analysis.

3. Recognition of metal ions by chemosensors 3 and 4

Chemosensors **3** and **4** (pH 7.0 ± 0.1; 10 mM HEPES in CH_3OH:H_2O, 3:1) exhibited λ_{max} at 492 and 490 nm, respectively, and on addition of Cu^{2+}(1 equiv.), new absorption band appeared at 615 nm and 600 nm, respectively, which induced a colour change from red to blue. The intensity of new absorption band increased gradually with the increase in concentration of Cu^{2+} (Figure 1) with simultaneous decrease in absorbance at λ_{max} 490/492 nm.

The spectral fitting of these data obtained by the titration of **3** and **4** with Cu^{2+} shows the formation

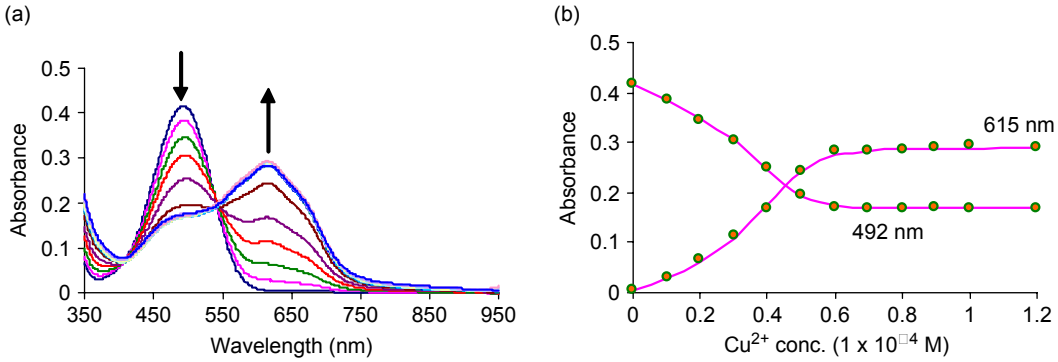

Figure 1. (a) Absorbance spectra of **3** (100 μM) on addition of different concentrations of Cu^{2+}; (b) plot of absorbance of **3** against Cu^{2+} conc. The points refer to experimental values and solid line refers to curve fitting.

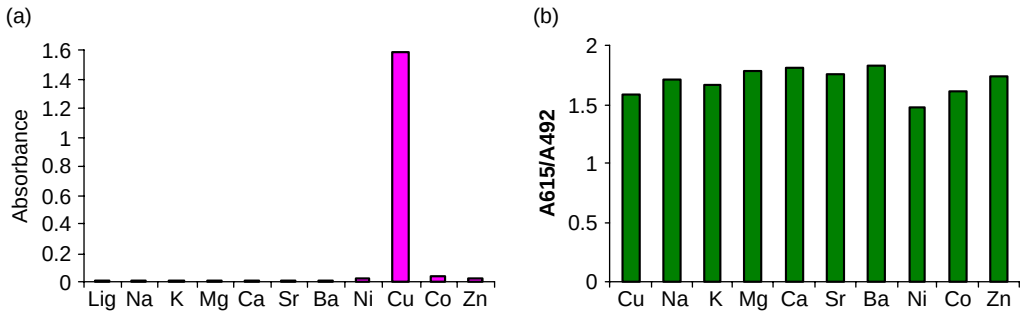

Figure 2. (a) Responses of chemosensor **3** (100 μM) to selected metal ions (100 μM); (b) spectrophotometric response of receptor **3** (100 μM) containing 100 μM Cu^{2+} to the selected metal ions (500 μM).

of mixture of complexes as described in Equations (1) and (2).

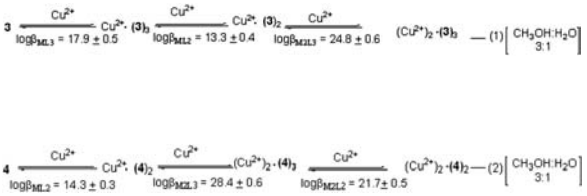

The disodium salt of the diacid **3** has an additional advantage of being freely soluble in water. The neutralisation of carboxylic acid of **3** does not affect the λ_{max}. The measurement of absorbance in the presence of various metal ions showed that only Cu^{2+} ions caused a notable response at 492 nm, whereas all other metal ions induced negligible responses. It is noteworthy that with Cu^{2+} ions a new band at longer wavelength, i.e. at 600 nm, was appeared. The evaluation of these spectral data shows the formation of ML_2 and ML_4 type of complexes (Equation (3)). However, the reasons for the formation of such higher stoichiometric species could not be rationalised.

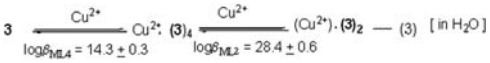

The addition of other metal ions to the solution of **3** such as Na^{+}, K^{+}, Mg^{2+}, Ca^{2+}, Sr^{2+}, Ba^{2+} and Cd^{2+} caused nominal changes in the absorption spectrum. However, addition of Ni^{2+} and Zn^{2+} showed lowering in absorption (10–15%) at 495 nm without the appearance of new absorption band, and addition of Co^{2+}, on prolonged standing (~12 h), resulted in a change in colour from red to blue. This is associated with a new red-shifted absorption band at 600 nm but with significantly lower epsilon value (ϵ 323) than observed in case of Cu^{2+}(ϵ 2070; Figure 2(a)). These metal ions, when present in large concentration, interfere in estimation of Cu^{2+}. Similar interference of transition metal ions in diacid-based Cu^{2+} receptor (*13f*) has been reported by Gunnlaugsson et al. earlier.

The addition of other metal ions, viz. Na^{+}, K^{+}, Mg^{2+}, Ca^{2+}, Sr^{2+}, Ba^{2+}, Co^{2+}, Ni^{2+} Zn^{2+} and Cd^{2+} to the solution of chemosensor **4** caused nominal changes in its absorption spectrum, and even their presence in large amounts (>100 times) did not affect the changes in absorbance arising due to addition of only Cu^{2+}. Therefore, chemosensor **4** shows higher selectivity towards Cu^{2+} than chemosensor **3**, but **4** has a limitation that due to its poor solubility, it cannot be used in the neat aqueous solution.

4. Stoichiometries and stability constants of the complexes as a function of pH

The influence of pH on the absorbance of **3** was determined by the UV–vis titration of CH_3OH:H_2O (3:1). The absorbance of **3** at 492 nm remained unaffected between pH 12.0 and 2.0 (Figure 3). On decreasing the pH below 8.0, a small hypsochromic shift (~15 nm) was observed. However, this hypsochromic shift did not result in any colour change of the solution.

Since this protonation process leads to only small changes in absorbance, any perturbation in λ_{max} and absorbance between pH 2.0 and 12.0 by the addition of an analyte in solution **3** could be attributed to interaction of the analyte with **3**.

In a similar manner, chemosensors **3** (in water) and **4** (CH_3OH:H_2O) showed pH-dependent nominal changes in

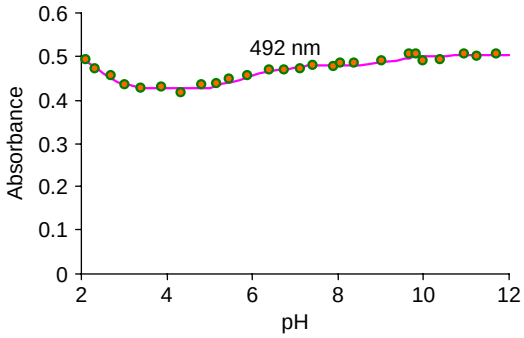

Figure 3. Plot of absorbance of **3** against pH.

Table 1. Log β values for protonation[a] of chemosensors **3** and **4** in different solvents.

Chemosensor	Log β_{LH}	Log β_{LH2}	Log β_{LH3}	Log β_{LH4}
3 (CH_3OH:H_2O, 3:1)	9.2 ± 0.02	15.1 ± 0.1	17.7 ± 0.2	20.2 ± 0.1
3 (H_2O)	9.0 ± 0.02	15.3 ± 0.2	20.2 ± 0.2	22.2 ± 0.3
4 (CH_3OH:H_2O, 1:1)	9.0 ± 0.04	14.3 ± 0.1	16.3 ± 0.1	–
4 (CH_3OH:H_2O, 3:1)	9.0 ± 0.03	14.3 ± 0.2	16.3 ± 0.2	–
4 (CH_3OH:H_2O, 1:2)	9.1 ± 0.03	15.9 ± 0.1	19.4 ± 0.2	–

[a] In case of **3**, L = dianion of **3** and in case of **4**, L = monoanion of **4**.

the absorption spectra accompanied by a small hypsochromic shift in the acidic region. The protonation constants (Table 1) and distribution of different species are affected by the solvent medium.

As Cu^{2+} binds with **3** and **4** to form different stoichiometric complexes other than 1:1 type of complex at pH 7.0, in order to avoid the complexity of results, the influence of pH on Cu^{2+} complexation with **3** and **4** was investigated by absorption measurements for 1:1 solutions of **3**−Cu^{2+} and **4**−Cu^{2+}. The plot of absorbance versus pH shows that at pH >4.0 the absorbance at 615 nm gradually increased and reached its limiting value at pH 8.5 in CH_3OH:H_2O (3:1) solution. In this pH range, the absorbance due to free **3** gradually decreased (Figure 4).

The simulation of these spectral data obtained from the combination of pH and UV–vis titration of **3** with Cu^{2+}(1:1) solution shows that at pH >4.0 the complexation of **3** with Cu^{2+} causes deprotonation at arylamine NH to form MLH_{-1} complex, and at pH >6.0 the formation of $MLH_{-1}(OH^-)$ complex starts, which gets completed at pH 8.5. Further addition of OH^- does not cleave this complex (Figure 5).

At pH <6.0, the formation of ML is initiated which shows its highest concentration at pH 4.0. On lowering the pH, ML undergoes protonation to form MLH (Equation (4)). The appearance of new absorption bands at 600 nm in case of MLH_{-1} and $MLH_{-1}(OH^-)$ species supports the deprotnation of aryl NH.

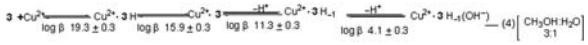

The titration of 1:1 solution of **3**–Cu^{2+} in H_2O exhibits λ_{max} at 615 nm at pH >5.0 which achieved limiting value at pH 8.5 (Figure 6). Lowering of pH <2.0 resulted in the reappearance of absorbance due to free **3**. Between pH 2.0 and 5.0, chemosensor **3** remains complexed with Cu^{2+} to form species which does not absorb at 615 nm. The formation of yellow solution of Cu^{2+}–**3** mixture at pH <5.0 confirms the formation of species with hypsochromic shift as against the free sensor **3**. The analysis of these data by spectral fitting shows the formation of MLH_{-1} and

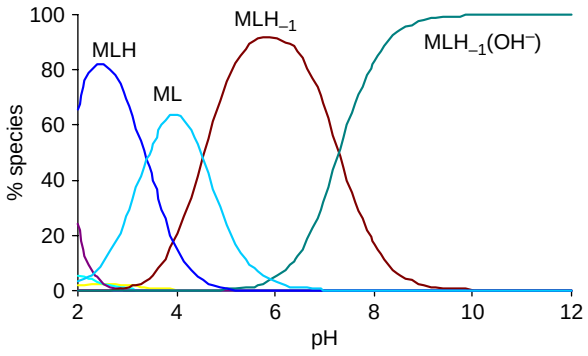

Figure 5. Species distribution diagram obtained from the pH titration of 1:1 solution of **3**–Cu^{2+} (100 μM).

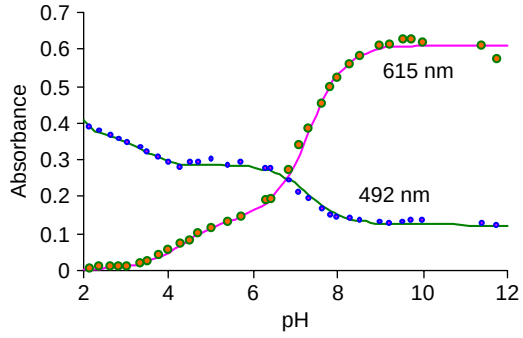

Figure 4. Plot of absorbances of **3**–Cu^{2+}(1:1, 100 μM) solution in CH_3OH:H_2O (3:1) at various pH values.

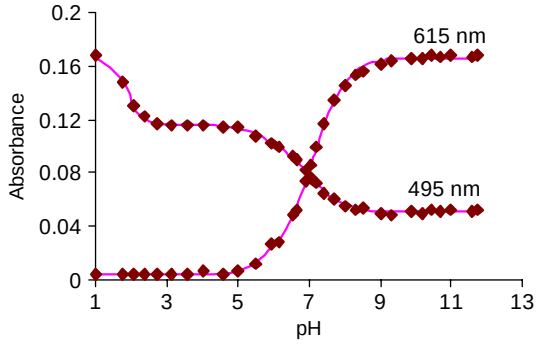

Figure 6. Plot of absorbances of **3**–Cu^{2+}(1:1, 100 μM) solution in H_2O.

Table 2. Log β values[a] of **3** and **4** with Cu^{2+} as a function of pH in different solvents.

Chemosensor	Log β_{MLH}	Log β_{ML}	Log β_{MLH-1}	Log $\beta_{MLH-1(OH-)}$
3 CH_3OH:H_2O, 3:1)	19.3 ± 0.3	15.9 ± 0.3	11.4 ± 0.3	4.1 ± 0.3
3 (H_2O)	21.5 ± 0.1	–	10.5 ± 0.1	3.4 ± 0.1
4 (CH_3OH:H_2O, 3:1)	–	11.2 ± 0.05	6.6 ± 0.1	1.3 ± 0.1
4 (CH_3OH:H_2O, 1:1)	–	11.8 ± 0.1	7.7 ± 0.1	1.4 ± 0.1
4 (CH_3OH:H_2O, 1:2)	–	12.5 ± 0.1	7.5 ± 0.1	4.0 ± 0.1

[a] In case of **3**, L = dianion of **3** and in case of **4**, L = monoanion of **4**.

$MLH_{-1}(OH^-)$ species at pH > 5.0. Formation of MLH species at pH < 5.0 is in consonance with apparent colour changes. These results are in parallel with the findings of complexation of **3** with Cu^{2+} in CH_3OH:H_2O mixture.

Chemosensor **4** showed poor solubility in water at low pH values, so studies were performed in various methanol–water mixtures. The titration of solutions of **4**–Cu^{2+}(1:1) between pH 2.0 and 12.0 and the analysis of these data through spectral simulation show the formation of ML, MLH_{-1} and $MLH_{-1}(OH^-)$ with varied distributions and stability constants in different media (Table 2, Figure 7). The absorbance versus pH plots show that the absorbance due to **4** at λ_{max} 492 nm decreases up to pH 5.0 and then achieves a plateau and remains stable between pH 6.0 and 12.0. The variation in absorbance arising due to **4**–Cu^{2+} complex at 615 nm significantly depends on the medium of solution. Absorbance remains stable at pH > 8.5 in CH_3OH:H_2O (3:1) and between pH 6.5 and 10.5 in CH_3OH:H_2O (1:2). Therefore, the change in absorbance at λ_{max} 492 nm between pH 5.0 and 12.0 can be used for the estimation of Cu^{2+}, and the change in absorbance at 615 nm, the new red-shifted absorption band, in CH_3OH:H_2O (1:2) between pH 6.0 and 11.0 can be used for the quantitative estimation of Cu^{2+}.

5. Dual behaviour of chemosensor 3 at two different pH values

The addition of Cu^{2+} to red solution of **3** at pH 3.0 or the addition of acid to blue solution of **3**–Cu^{2+} at pH 7.0 resulted in yellow solution, which gave absorption band at 465 nm in their UV–vis spectra. These experiments confirm the dual binding mode of receptor **3** towards Cu^{2+} depending on pH. At pH 7.0, Cu^{2+} binds with **3** to give

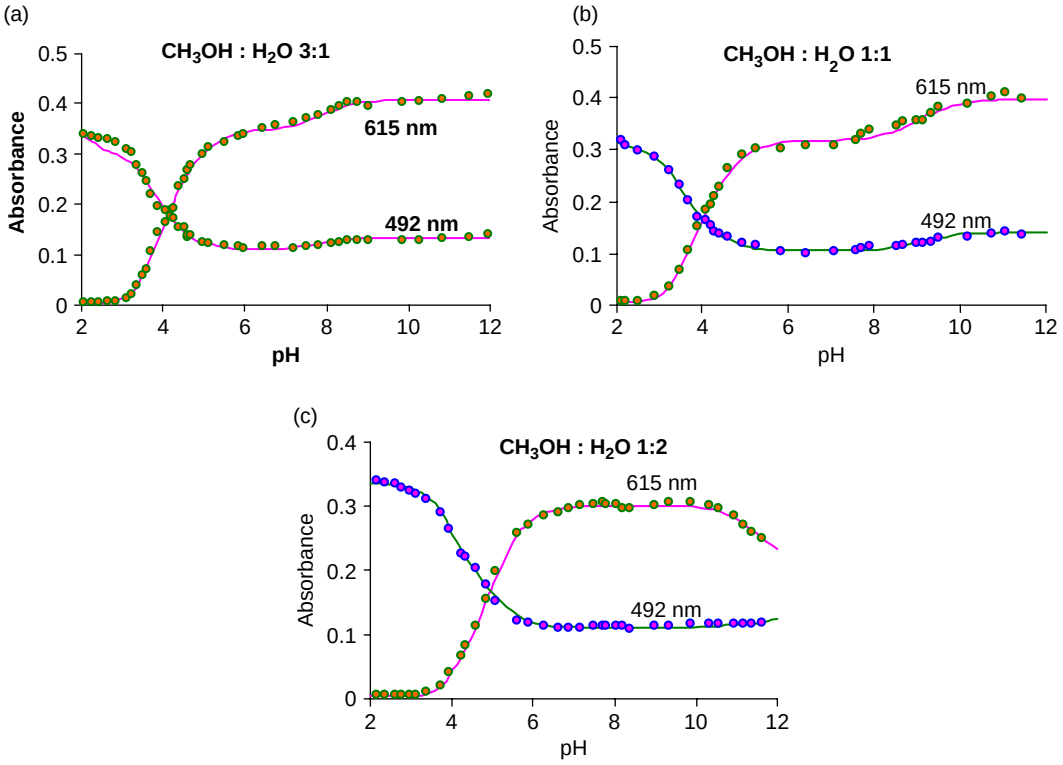

Figure 7. Plot of absorbances of **4**–Cu^{2+}(1:1) solution as a function of pH in the solvent system: (a) CH_3OH:H_2O (3:1); (b) CH_3OH:H_2O (1:1); (c) CH_3OH:H_2O (1:2).

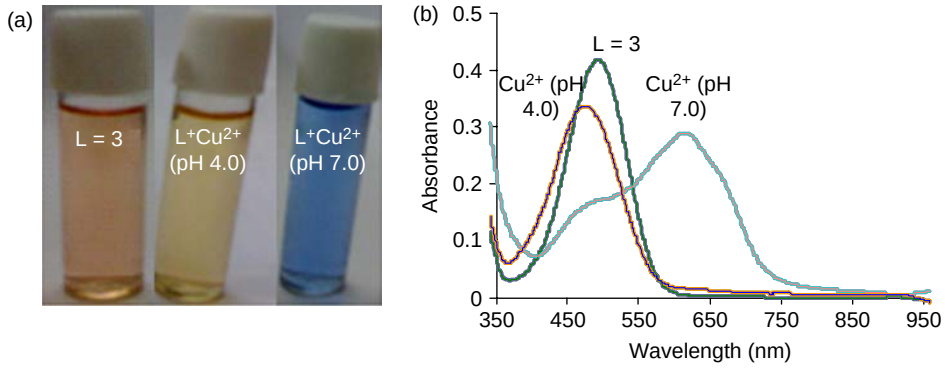

Figure 8. (a) Visual colour changes; (b) spectral responses of sensor **3** on addition of Cu^{2+} at pH 7.0 and 4.0.

red-shifted absorbance, and at pH 4.0, it causes hypsochromic shift (Figure 8). These results clearly point that the elaboration of additional binding sites on anthraquinone moiety and the control of hydrophilic/hydrophobic nature of the groups effectively control the binding modes.

6. Elaboration of molecular photonic logic systems

Molecular switches and logic gates are analogous because both convert input stimulations into output signals with intrinsic protocols. It follows that the principles of binary logic can be applied to the signal transduction operated by molecular switches. The analysis of their logic behaviours requires, first of all, the assignment of threshold values and logic convention to their inputs and outputs signals.

6.1 Combination of Cu^{2+} and H^+ driven logic gates

Chemosensor **3** exhibits a unique logic gate system that involves an 'INHIBIT' (*19*) gate as described in Figure 9 via the combination of two input signals, Cu^{2+} (input 1) and protonation (input 2) in CH_3OH:H_2O (3:1). The input can take values of 0 and 1 corresponding to the absence or the presence of action. The output, the absorbance at a given wavelength, can be of values 0 and 1 depending on the absorbance value below or above a certain threshold. (Here, threshold value is 0.0184.) The vertical line shows wavelength (615 nm) at which the observed signal results in 'INHIBIT' molecular logic device (Figure 9(x)). This logic device processes input signals according to the truth table shown in Figure 9(y).

6.2 Combination of Cu^{2+} and OH^- driven logic gates

The evaluation of stimulations due to Cu^{2+} and OH^- as two inputs results in 'TRANSFER' (*20*) logic at $\lambda = 615$ nm (Figure 10).

'TRANSFER' logic requires the signal to be '0' when both inputs are '0' and also when only one of the inputs is '1'. However, when the other input is '1' or when both are '1', the output is '1'. The free **3** (100 μM; *A* 0.003) and addition of OH^- (pH 10.0; *A* 0.01) lead to low output at 615 nm. High output ('1'; *A* 0.28) has been found only in the presence of Cu^{2+} (pH 7.0) and remains high even after the addition of both Cu^{2+} and OH^- (both at pH 10.0; *A* 0.61; Figure 10).

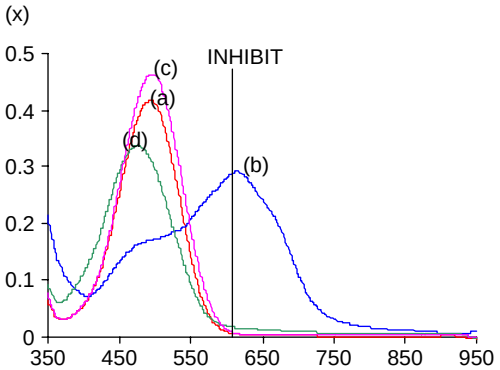

(y)

	Cu^{2+}	H^+	OUT 615nm	
	0	0	0	
pH 7.0	1	0	1	INHIBIT
pH 4.0	0	1	0	
pH 4.0	1	1	0	

Figure 9. (x) Molecular scale implementation of logic gates: (a) blank; (b) **3** + Cu^{2+} (pH 7.0); (c) **3** + H^+ (pH 4.0); (d) **3** + Cu^{2+} + H^+ (pH 4.0). (y) Truth table for 'INHIBIT' logical gate performance.

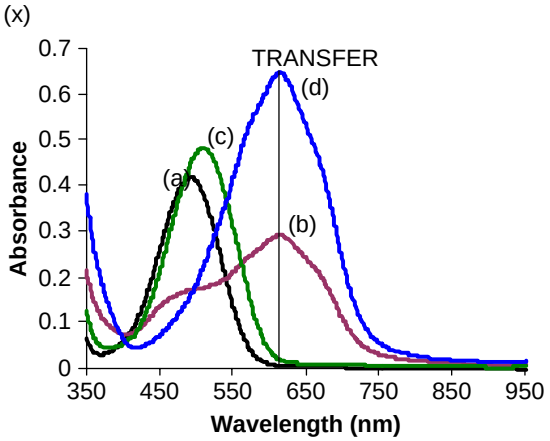

(y)

	Cu^{2+}	OH^-	OUT 615nm	
	0	0	0	TRANSFER
pH 7.0	1	0	1	
pH 10.0	0	1	0	
pH 10.0	1	1	0	

Figure 10. (x) Molecular scale implementation of logic gates: (a) blank; (b) **3** + Cu^{2+} (pH 7.0); (c) **3** + OH^- (pH 10.0); (d) **3** + Cu^{2+} + OH^- (pH 10.0). (y) Truth table for 'TRANSFER' logical gate performance.

7. Conclusions

Herein, we have presented carboxylic acid–diamine-based chromogenic sensors that showed characteristic UV–vis spectral changes and drastic colour changes upon addition of Cu^{2+}. Particularly, chemosensor **3** showed the property of absorption/colour changes in neat aqueous solution, which is a prerequisite for their use in biological environment. Insight into the spectral responses revealed that these changes arise due to selective deprotonation of aryl amine NH by Cu^{2+}. Also, chemosensor **3** exhibits a unique logic gate system that involves 'INHIBIT' and 'TRANSFER' logic gates.

8. Experimental

8.1 Materials and methods

Melting points were determined in capillaries and are uncorrected. ^{1}H NMR spectra were recorded on JEOL Al 300 MHz instrument using $CDCl_3$ solution containing tetramethylsilane (TMS) as an internal standard. The chemical shifts are reported in δ values relative to TMS and coupling constants (J) are expressed in hertz. ^{13}C NMR spectra were recorded at 75 MHz and values are reported relative to $CDCl_3$ signal at δ 77.0. Chromatography was performed with silica gel 100–200 mesh and the reactions were monitored by thin layer chromatography with glass plates coated with silica gel HF-254. FAB mass spectra were recorded as normal ion (MF linear).

8.2 General procedure for the synthesis of chemosensors 3 and 4

To a solution of 1-(2-amionoethylamino)anthracene-9, 10-dione (532 mg, 2 mmol) in CH_3CN, K_2CO_3 (828 mg, 6 mmol) and ethyl bromoacetate (668 mg, 8 mmol) were added. The reaction mixture was stirred at 80°C for 6 h. The solvent was removed under vacuum and the residue was partitioned between dichloromethane and water. The organic phase was washed with water (3 × 50 mL) and then dried (Na_2SO_4). The crude product was chromatographed on silica gel (100–200 mesh) to give pure diester **1** (higher R_f component, red solid) and monoester **2** (lower R_f component). Then compound **1** (438 mg, 1 mmol) was hydrolysed with 10% NaOH (120 mg, 3 mmol) in ethanol for 5 h. After concentrating the reaction mixture, the residue was poured to crushed ice. The solid formed was filtered off and crystallised from ethanol to give pure **3**. Similarly, the hydrolysis of monoester **2** with NaOH in ethanol resulted in formation of compound **4**.

8.3 Chemosensor 1

Red solid; 60%; m.p. 78°C; FAB mass M^+m/z 439 ($M^+ + 1$); IR υ_{max} (KBr) 1726, 1751 and 3473 cm^{-1}; ^{1}H NMR ($CDCl_3$): δ 1.28 (t, $J = 7.2$ Hz, 6H, 2 × CH_3), 3.16 (t, $J = 6.6$ Hz, 2H, CH_2), 3.49 (q, $J = 4.5$ Hz, 4H, 2 × CH_2), 3.67 (s, 4H, 2 × CH_2), 4.19 (q, $J = 7.2$ Hz, 2H, CH_2), 7.10 (d, $J = 8.4$ Hz, 1H, ArH), 7.53–7.62 (m, 2H, ArH), 7.68–7.79 (m, 2H, ArH), 8.22–8.31 (m, 2H, ArH) and 9.84 (bs, 1H, NH, exchanges with D_2O); ^{13}C NMR (normal/DEPT-135) ($CDCl_3$): δ 14.18 (CH_3), 41.14 (CH_2), 52.81 (CH_2), 55.27 (CH_2), 60.86 (CH_2), 107.71 (C), 115.83 (CH), 117.85 (CH), 126.66 (CH), 126.77 (CH), 132.91 (CH), 133.90 (CH), 134.67 (C), 134.92 (C), 135.31 (CH), 140.42 (C), 151.35 (C), 170.69 (C), 183.84 (C) and 184.91 (C); Found C 65.98; H 5.75; N 6.28% $C_{24}H_{26}N_2O_6$ requires C 65.74; H 5.98; N 6.39%.

8.4 Chemosensor 2

Red solid; 30%; m.p. 68°C; FAB mass M^+m/z 353 ($M^+ + 1$); ^{1}H NMR ($CDCl_3$): δ 0.87 (t, $J = 6.9$ Hz, 3H,

CH_3), 3.05 (s, 2H, CH_2), 3.51 (t, $J = 6.0$ Hz, 2H, CH_2), 3.63 (q, $J = 6.0$ Hz, 2H, CH_2), 4.72 (q, $J = 6.9$ Hz, 2H, CH_2), 7.13 (d, $J = 8.1$ Hz, 1H, ArH), 7.56–7.70 (m, 2H, ArH), 7.72–7.80 (m, 2H, ArH), 8.23–8.28 (m, 2H, ArH) and 9.87 (bs, 1H, NH, exchanges with D_2O); ^{13}C NMR (normal/DEPT-135) ($CDCl_3$): δ 13.80 (CH_3), 41.04 (CH_2), 51.61 (CH_2), 54.27 (CH_2), 60.56 (CH_2), 110.71 (C), 115.53 (CH), 118.05 (CH), 126.26 (CH), 126.97 (CH), 133.11 (CH), 133.69 (CH), 134.17 (C), 135.38 (C), 135.91 (CH), 141.42 (C), 151.25 (C), 170.60 (C), 183.14 (C) and 184.81 (C); Found C 68.38; H 5.95; N 7.68% $C_{20}H_{20}N_2O_4$ requires C 68.17; H 5.72; N 7.95%.

8.5 Chemosensor 3

Red solid, 60%; m.p. 185°C (ethanol); FAB mass M^+*m*/*z* 383 ($M^+ + 1$); IR υ_{max} (KBr) 1632, 1676, 1728 and 3284 cm^{-1}; ^{1}H NMR ($CDCl_3$ + DMSO-d_6): δ 3.42 (bs, 2H, CH_2), 3.75 (bs, 2H, CH_2), 4.10 (bs, 4H, 2 × CH_2), 7.32 (d, $J = 8.4$ Hz, 1H, ArH), 7.48 (d, $J = 7.2$ Hz, 1H, ArH), 7.63 (t, $J = 8.4$ Hz, 1H, ArH), 7.79–7.90 (m, 2H, ArH), 8.11–8.27 (m, 2H, ArH) and 9.71 (bs,1H, NH); ^{13}C NMR (normal/DEPT135) ($CDCl_3$–DMSO-d_6): δ 38.19 (CH_2), 53.50 (CH_2), 54.52 (CH_2), 112.68 (C), 115.24 (CH), 118.22 (CH), 126.06 (CH), 126.25 (CH), 132.19 (C), 133.17 (CH), 133.94 (C), 134.14 (CH), 135.28 (CH), 150.60 (C), 168.83 (C), 182.61 (C) and 183.83 (C); Found C 62.80; H 4.73; N 7.35% $C_{20}H_{18}N_2O_6$ requires C 62.82; H 4.74; N 7.33%.

8.6 Chemosensor 4

Red solid, 55%; m.p. 230°C (ethanol); FAB mass M^+*m*/*z* 324 ($M^+ + 1$); ^{1}H NMR ($CDCl_3$ + DMSO-d_6): δ 3.78 (bs, 2H, CH_2), 4.01 (bs, 2H, CH_2), 4.25 (bs, 2H, CH_2), 7.73 (bs, 1H, ArH), 7.87 (bs, 4H, ArH), 8.09 (bs, 1H, ArH) and 8.29 (bs, 1H, ArH); ^{13}C NMR (normal/DEPT-135) ($CDCl_3$–DMSO-d_6): δ 40.38 (CH_2), 47.99 (CH_2), 48.50 (CH_2), 114.89 (CH), 120.13 (CH), 120.57 (CH), 127.19 (CH), 127.91 (C), 132.68 (C), 133.93 (C), 134.72 (CH), 135.11 (CH), 135.72 (C), 137.34 (CH), 152.62 (C), 172.65 (C), 185.27 (C) and 187.17 (C); Found C 66.80; H 4.73; N 8.45% $C_{18}H_{16}N_2O_4$ requires C 66.66; H 4.97; N 8.64%.

8.7 Photophysical studies

All the solvents were of analytic grade and used after distillation. The solutions of metal ions were prepared in distilled water. All pH measurements were made with Equiptronics pH meter. UV–vis spectroscopy experiments were carried out on a Shimadzu UV-1601 PC by using slit widths of 1.0 nm and matched quartz cells. All absorption scans were saved as ACS II files and further processed in Excel™ to produce all graphs shown. Cu^{2+}-binding characteristics and affinity and stoichiometries of different complexes were assessed via titrations with $Cu(NO_3)_2$. Titration data are fit with programme Specfit/32, which analyses multi-wavelength data using an iterative method to obtain the association constant in terms of free or unbound Cu^{2+}.

Acknowledgements

We thank CSIR and DST, New Delhi, for their financial assistance.

Note

1. Email: subodh_gndu@yahoo.co.in

References

(1) (a) Vauer, B., Ed. *Molecular Fluorescence: Principles and Applications*; Wiley-VCH: Weinheim, Germany, **2002**. (b) Feringa, B.L., Ed. *Molecular Switches*; Wiley-VCH: Weinheim, Germany, **2001**.

(2) Haugland, R.P. *Handbook of Fluorescent Probes and Research Chemical*, 9th ed. Molecular Probes, Inc. Eugene, OR, 2002.

(3) de Silva, A.P.; Gunaratne, H.Q.N.; Gunnlaugsson, T.; Huxley, A.J.M.; McCoy, C.P.; Rademacher, J.T.; Rice, T.E. *Chem. Rev.* **1997**, *97*, 1515–1566.

(4) (a) Sessler, J.L.; Gale, P.A.; Cho, W.S. *Anion Receptor Chemistry*; Royal Society of Chemistry: Cambridge, UK, **2006**. (b) Gunnlaugsson, T.; Glynn, M.; Tocci, G.M. (nee Hussey); Kruger, P.E.; Pfeffer, F.M. *Coord. Chem. Rev.* **2006**, *250*, 3094–3117. (c) Martinez-Manez, R.; Sancenon, F. *Chem. Rev.* **2003**, *103*, 4419–4476. (d) Prados, P.; Quesada, R. *Supramol. Chem.* **2008**, *20*, 201–216. (e) Gale, P.A.; Quesada, R. *Coord. Chem. Rev.* **2006**, *250*, 3219–3244. (f) Martınez-Manez, R.; Sancenon, F. *J. Fluoresc.* **2005**, *15*, 267–285. (g) Gale, P.A.; Garcıa-Garrido, S.E.; Garric, J. *Chem. Soc. Rev.* **2008**, *37*, 151–190. (h) Caltagirone, C.; Gale, P.A. *Chem. Soc. Rev.* **2009**, *38*, 520–563.

(5) (a) Welz, B.; Sperling, M. *Atomic Absorption Spectrometry*; Wiley-VCH: Weinheim, **1999**. (b) Taylor, H.E. *Inductively Coupled Plasma Mass Spectrometry: Practices And Techniques*; Academic Press: San Diego, CA, **2000**.

(6) For recent examples see: (a) Nishiyabu, R.; Anzenbacher, P. Jr. *J. Am. Chem. Soc.* **2005**, *127*, 8270–8271. (b) Ali, H. D.P.; Kruger, P.E.; Gunnlaugsson, T. *New J. Chem.* **2008**, *32*, 1153–1161. (c) Gunnlaugsson, T.; Kruger, P.E.; Jensen, P.; Tierney, J.; Ali, H.D.P.; Hussey, G.M.*J. Org. Chem.* **2005**, *70*, 10875–10878. (d) Basurto, S.; Riant, O.; Moreno, D.; Rojo, J.; Torroba, T.*J. Org. Chem.* **2007**, *72*, 4673–4688. (e) Suksai, C.; Tuntulani, T. *Chem. Soc. Rev.* **2003**, *32*, 192–202. (f) Caballero, A.; Martinez, R.; Lloveras, V.; Ratera, I.; Vidal-Gancedo, J.; Wurst, K.; Tarraga, A.; Molina, P.; Veciana, J.*J. Am. Chem. Soc.* **2005**, *127*, 15666–15667. (g) Molina, P.; Tarraga, A.; Caballero, A. *Eur. J. Inorg. Chem.* **2008**, 3401–3417. (h) Batista, R.M.F.; Oliveira, E.; Costa, S.P.G.; Lodeiro, C.; Raposo, M.M.M. *Org. Lett.* **2007**, *9*, 3201–3204. (i) Ballesteros, E.; Moreno, D.; Gomez, T.; Rodriguez, T.; Rojo, J.; Garcıa-Valverde, M.; Torroba, T. *Org. Lett.* **2009**, *11*, 1269–1272.

(7) Lee, S.; Choi, I.; Hong, S.; Yang, Y.I.; Lee, J.; Kang, T.; Yi, J. *Chem. Commun.* **2009**, *41*, 6171–6173.

(8) (a) Gaggelli, E.; Kozlowski, H.; Valensin, D.; Valensin, G. *Chem. Rev*. **2006**, *106*, 1995–2044. (b) Uauy, R.; Olivares, M.; Gonzalez, M. *Am. J. Clin. Nutr.* **1998**, *67*, 952S–959S.

(9) Kramer, R. *Angew. Chem. Int. Ed.* **1998**, *37*, 772–773.

(10) Georgopoulos, P.G.; Roy, A.; Yonone-Lioy, M.J.; Opiekun, R.E.; Lioy, P.J. *J. Toxicol. Environ. Health, B* **2001**, *4*, 341–394.

(11) (a) Zheng, Y.J.; Orbulescu, J.; Ji, X.J.; Andreopoulos, F.M.; Pham, S.M.; Leblanc, R.M.*J. Am. Chem. Soc.* **2003**, *125*, 2680–2686. (b) Ocypa, M.; Michalska, A.; Maksymiuk, K. *Electrochim. Acta* **2006**, 2298–2305. (c) Mashhadizadeh, M.H.; Zadmehr, M.R.; Allah-Abadi, H. *Asian J. Chem.* **2006**, *18*, 137–144. (d) Yang, K.X.; Swami, K.; Husain, L. *Spectrochim. Acta, B* **2002**, *57*, 73–84.

(12) (a) Shao, N.; Zhang, Y.; Cheung, S.M.; Yang, R.H.; Chan, W.H.; Mo, T.; Li, K.A.; Liu, F. *Anal. Chem.* **2005**, *77*, 7294–7303. (b) Yu, M.X.; Shi, M.; Chen, Z.G.; Li, F.Y.; Li, X.X.; Gao, Y.H.; Xu, J.; Yang, H.; Zhou, Z.G.; Yi, T.; Huang, C.H. *Chem. Eur. J.* **2008**, *14*, 6892–6900. (c) Domaille, D.W.; Que, E.L.; Chang, C.J. *Nat. Chem. Biol.* **2008**, *4*, 168–175. (d) Swamy, K.M.K.; Ko, S.K.; Kwon, S.K.; Lee, H.N.; Mao, C.; Kim, J.M.; Lee, K.H.; Kim, J.; Shin, I.; Yoon, J. *Chem. Commun.* **2008**, 5915–5917. (e) Jung, H.S.; Kwon, P.S.; Lee, J.W.; Kim, J.I.; Hong, C.S.; Kim, J.W.; Yan, S.H.; Lee, J.Y.; Lee, J.H.; Joo, T.; Kim, J.S. *J. Am. Chem. Soc.* **2009**, *131*, 2008–2012. (f) Zhou, Y.; Wang, F.; Kim, Y.; Kim, S.J.; Yoon, J. *Org. Lett.* **2009**, *11*, 4442–4445.

(13) Recent references: (a) Zhao, Y.; Zhang, X.B.; Han, Z.X.; Qiao, L.; Li, C.Y.; Jian, L.X.; Shen, G.L.; Yu, R.Q. *Anal. Chem.* **2009**, *81*, 7022–7030. (b) Huang, J.; Xu, Y.; Qian, X. *Dalton. Trans.* **2009**, 1761–1766. (c) Chen, X.Q.; Jou, M.J.; Lee, H.; Kou, S.Z.; Lim, J.; Nam, S.W.; Park, S.; Kim, K.M.; Yoon, J. *Sens. Actuators, B* **2009**, *137*, 597–602. (d) Rodriguez-Morgade, M.S.; Planells, M.; Torres, T.; Ballester, P.; Palomares, E. *J. Mater. Chem.* **2008**, *18*, 176–181. (e) Martinez, R.; Zapata, F.; Caballero, A.; Espinosa, A.; Tarraga, A.; Molina, P. *Org. Lett.* **2006**, *8*, 3235–3238. (f) Gunnlaugsson, T.; Leonard, J.P.; Murray, N.S. *Org. Lett.* **2004**, *6*, 1557–1560. (g) Shao, N.; Jin, J.Y.; Wang, H.; Zhang, Y.; Yang, R.H.; Chan, W.H. *Anal. Chem.* **2008**, *80*, 3466–3475. (h) Moletti, A.; Coluccini, C.; Pasini, D.; Taglietti, A. *Dalton. Trans.* **2007**, 1588–1592. (i) Sheng, R.L.; Wang, P.F.; Gao, Y.H.; Wu, Y.; Liu, W.M.; Ma, J.J.; Li, H.P.; Wu, S.K. *Org. Lett.* **2008**, *10*, 5015–5018. (j) Xiang, Y.; Li, M.; Chen, X.T.; Tong, A.J. *Talanta* **2008**, *74*, 1148–1153. (k) Mashraqui, S.H.; Khan, T.; Sundaram, S.; Ghadigaonkar, S. *Tetrahedron Lett.* **2008**, *49*, 3739–3743. (l) Kim, M.H.; Noh, J.H.; Kim, S.; Ahn, S.; Chang, S.K. *Dyes Pigm.* **2009**, *82*, 341–346.

(14) (a) Valuer, B.; Leray, I. *Coord. Chem. Rev.* **2000**, *205*, 3–40. (b) de Silva, A.P.; Gunaratne, H.Q.N.; Gunnlaugsson, T.; Huxley, A.J.M.; McCoy, C.P.; Rademacher, J.T.; Rice, T.E. *Chem. Rev.* **1997**, *97*, 1515–1566. (c) Descalzo, A.B.; Martinez-Manez, R.; Sancenon, F.; Hoffmann, K.; Rurack, K. *Angew Chem.* **2006**, *118*, 6068–6093. (d) Martinez-Manez, R.; Sancenon, F. *Coord. Chem. Rev.* **2006**, *250*, 3081–3093. (e) Martinez-Manez, R.; Sancenon, F.*J. Fluoresc.* **2005**, *15*, 267–285. (f) Wiskur, S.L.; Ait-Haddou, H.; Lavigne, J.J.; Anslyn, E.V. *Acc. Chem. Res.* **2001**, *34*, 963–972.

(15) (a) Magri, D.C.; Vance, T.P.; de Silva, A.P. *Inorg. Chim. Acta* **2007**, *360*, 751–764. (b) de Silva, A.P.; Leydet, Y.; Lincheneau, C.; McClenaghan, N.D.*J. Phys. Condens. Matter* **2006**, *18*, S1847–S1872. (c) Balzani, V.; Credi, A.; Venturi, M. *Chem. Phys. Chem.* **2003**, *4*, 49–59. (d) Raymo, F.M. *Adv. Mater.* **2002**, *14*, 401–414. (e) Ramyo, F.M.; Giordani, S.*J. Am. Chem. Soc.* **2002**, *124*, 2004–2007. (f) Margulies, D.; Melman, G.; Shanzer, A.J. *Am. Chem. Soc.* **2006**, *128*, 4865–4871.

(16) (a) Miyaji, H.; Sessler, J.L. *Angew. Chem. Int. Ed.* **2001**, *40*, 154–157. (b) Miyaji, H.; Sato, W.; Sessler, J.L. *Angew. Chem. Int. Ed.* **2000**, *39*, 1777–1780. (c) Jimenez, D.; Martinez-Manez, R.; Sancenon, F.; Soto, J. *Tetrahedron Lett.* **2002**, *43*, 2823–2825. (d) Jose, D.A.; Kumar, D.K.; Ganguly, B.; Das, A. *Org. Lett.* **2004**, *6*, 3445–3448.

(17) (a) Kumar, S.; Kaur, N. *Supramolecular Chem.* **2006**, *18*, 137–140. (b) Kaur, N.; Kumar, S. *Dalton Trans.* **2006**, 3766–3771. (c) Kaur, N.; Kumar, S. *Tetrahedron* **2008**, *64*, 3168–3175. (d) Kaur, N.; Kumar, S. *Tetrahedron Lett.* **2006**, *47*, 4109–4112. (e) Kaur, N.; Kumar, S. *Chem. Commun.* **2007**, 3069–3070. (f) Kaur, N.; Kumar, S. *Tetrahedron Lett.* **2008**, *49*, 5067–5069.

(18) (a) Xu, Z.; Xiao, Y.; Qian, X.; Cui, J.; Cui, D. *Org. Lett.* **2005**, *7*, 889–892. (b) Huang, J.; Xu, Y.; Qian, X. *Dalton Trans*. **2009**, 1761–1766. (c) Huang, J.; Xu, Y.; Qian, X. *Org. Biomol. Chem.* **2009**, *7*, 1299–1303. (d) Xu, Z.; Pan, J.; Spring, D.R.; Cui, J.; Yoon, J. *Tetrahedron* **2010**, *66*, 1678–1683.

(19) (a) Gunnlaugsson, T.; MacDonail, D.A.; Parker, D. *J. Chem. Soc. Chem. Commun.* **2000**, *93*. (b) Montenegro, J.-M.; Perez-Inestrosa, E.; Collado, D.; Vida, Y.; Suau, R. *Org. Lett.* **2004**, *6*, 2353–2355.

(20) Baytekin, H.T.; Akkaya, E.U. *Org. Lett.* **2000**, *2*, 1725–1727.